A High-Frequency Low-Power Low-Pass-Filter-Based All-Current-Mirror Sinusoidal Quadrature Oscillator

A. Leelasantitham, and B. Srisuchinwong

***Abstract*—**A high-frequency low-power sinusoidal quadrature oscillator is presented through the use of two 2nd-order low-pass current-mirror (CM)-based filters, a 1st-order CM low-pass filter and a CM bilinear transfer function. The technique is relatively simple based on (i) inherent time constants of current mirrors, i.e. the internal capacitances and the transconductance of a diode-connected NMOS, (ii) a simple negative resistance R_N formed by a resistor load R_L of a current mirror. Neither external capacitances nor inductances are required. As a particular example, a 1.9-GHz, 0.45-mW, 2-V CMOS low-pass-filter-based all-current-mirror sinusoidal quadrature oscillator is demonstrated. The oscillation frequency (f_0) is 1.9 GHz and is current-tunable over a range of 370 MHz or 21.6 %. The power consumption is at approximately 0.45 mW. The amplitude matching and the quadrature phase matching are better than 0.05 dB and 0.15°, respectively. Total harmonic distortions (THD) are less than 0.3 %. At 2 MHz offset from the 1.9 GHz, the carrier to noise ratio (CNR) is 90.01 dBc/Hz whilst the figure of merit called a normalized carrier-to-noise ratio (CNR_{norm}) is 153.03 dBc/Hz. The ratio of the oscillation frequency (f_0) to the unity-gain frequency (f_T) of a transistor is 0.25. Comparisons to other approaches are also included.

***Keywords*—**Sinusoidal quadrature oscillator, low-pass-filter-based, current-mirror bilinear transfer function, all-current-mirror, negative resistance, low power, high frequency, low distortion.

I. INTRODUCTION

QUADRATURE oscillators (QOs) typically provide two sinusoids with 90° phase difference for a variety of applications such as in receivers for wireless communication systems (GSM, PCS or Bluetooth etc). For example, GSM 1800-MHz or PCS 1.9-GHz receivers require operating frequencies between 1.805 to 1.99 GHz [1]. QOs are important for receivers and examples of reasons are as follows:

a) Hartley and Weaver image-reject receivers [2], superheterodyne receivers [3], zero-intermediate frequency (zero-IF) or direct-conversion receivers [4], low-IF [5], digital IF [3] receivers and direct digital or digital RF receivers [3] employ the quadrature downconverter.
b) Double low-IF and wide-band IF receivers [3] employ the double quadrature downconverter.

Generally, QOs can be either non-linear or linear types. Non-linear QOs such as relaxation and ring QOs are usually realized using periodically switching mechanisms and therefore outputs may not be readily low-distortion sinusoids [6]. In contrast, linear QOs employ frequency-selective networks such as RC or LC circuits and consequently low-distortion sinusoids can be readily generated [7].

As mentioned earlier, the required operating frequencies between 1.805 to 1.99 GHz in the receivers are typically utilized in the GSM 1800 MHz or PCS 1.9 GHz [1]. In the well open literature, no other linear (sinusoidal) QOs using RC techniques have been reported for tuning ranges of high oscillation frequencies from 1.805 to 1.99 GHz. Existing RC techniques for QOs include all-pass filters [8], operational transconductance amplifiers using capacitors (OTA-C) [9], operational transresistance amplifiers (OTRA) [10], current conveyers [11] and negative resistance [7]. Related attempts to use BJT current mirrors (CMs) have been reported but only for RC non-quadrature oscillators [12], [13].

Such RC techniques have suffered not only from relatively low oscillation frequencies between 40 kHz to 8 MHz due to the use of relatively large off-chip capacitors but also from relatively high power consumptions. However, existing RC linear QOs exploiting techniques using internal capacitances of either BJTs [14] or MOS [15] have been demonstrated for high oscillation frequencies at 0.58 GHz [14] and 2.83 GHz [15], whilst their oscillation frequencies are not tuned in the range from 1.805 to 1.99 GHz.

Alternative LC techniques using CMOS [16], [17], [18] offer high oscillation frequencies between 1.8 to 1.97 GHz whilst their power consumptions are relatively high between 15 to 50 mW. Recently, non-linear QOs have exploited techniques using internal capacitances of either MOS [19], [20] or BJTs [21], [22] for high oscillation frequency between 1.8 to 2.5 GHz. However, the ratios of the oscillation frequency (f_0) to the unity-gain frequency (f_T) [7] of a transistor are in the region of 0.1 to 0.2 whilst the power

The authors are grateful to The Thailand Research Fund (TRF) for the research grant of The Royal Golden Jubilee Program.

A. Leelasantitham is with School of Engineering, University of the Thai Chamber of Commerce, 126/1, Vibhavadee-Rangsit Road, Dindaeng, Bangkok 10400, Thailand, (corresponding author to provide phone: (+66 2) 697-6721; fax: (+66 2) 275-4892; e-mail: adisorn_lee@utcc.ac.th, leeadisorn@yahoo.com).

B. Srisuchinwong is with School of Communications, Instrumentation and Control Systems, Sirindhorn International Institute of Technology, Bangkadi, Thammasat University, 160 Moo 5, Tiwanont Road, Bangkadi, Muang Pathumtani, 12000, Thailand.

consumptions are relatively high between 7.01 to 100 mW.

In this paper, a high-frequency low-power all-current-mirror sinusoidal quadrature oscillator using two 2nd-order low-pass CM-based filters, a 1st-order CM low-pass filter and a CM bilinear transfer function. The technique is relatively simple based on (i) inherent time constants of current mirrors, i.e. the internal capacitances and the transconductance of a diode-connected NMOS, (ii) a simple negative resistance R_N formed by a resistor load R_L of a current mirror. Neither external capacitances nor inductances are required.

As a particular example, a 1.9-GHz, 0.45-mW, 2-V, CMOS low-pass-filter-based all-current-mirror sinusoidal quadrature oscillator is demonstrated. The oscillation frequency (f_0) is 1.9 GHz and is current-tunable over a range of 370 MHz or 21.6 %. The power consumption is at approximately 0.45 mW. The amplitude matching and the quadrature phase matching are better than 0.05 dB and 0.15°, respectively. Total harmonic distortions (THD) are less than 0.3 %. At 2 MHz offset from the 1.9 GHz, the carrier to noise ratio (CNR) is 90.01 dBc/Hz whilst the figure of merit called a normalized carrier-to-noise ratio (CNR_{norm}) is 153.03 dBc/Hz. The ratio of the oscillation frequency (f_0) to the unity-gain frequency (f_T) of a transistor is 0.25. Comparisons to other approaches are also included.

II. Proposed Techniques

A. Circuit Descriptions

Figs. 1 and 2 show the small-signal block diagrams and the circuit configuration, respectively, of the 1.9-GHz, 0.45-mW, 2-V CMOS low-pass-filter-based all-current-mirror sinusoidal quadrature oscillator. As shown in Fig. 1, the circuit for the low-pass-filter-based technique consists of four simple cascaded current-mirror (CM) filters connected together in a close loop as follows:

(a) a 2nd-order low-pass CM-based filter F_1 consists of
 (a.1) a 1st-order CM low-pass filter (LPF) F'_1 formed by a current mirror (Q_1, Q_2),
 (a.2) a 1st-order CM low-pass filter (LPF) F'_2 formed by a current mirror (Q_3, Q_4),
(b) a 2nd-order low-pass CM-based filter F_2 consists of
 (b.1) a 1st-order CM low-pass filter (LPF) F'_3 formed by a current mirror (Q_5, Q_6),
 (b.2) a 1st-order CM low-pass filter (LPF) F'_4 formed by a current mirror (Q_7, Q_8),
(c) a 1st-order CM low-pass filter (LPF) F_3 formed by a current mirror (Q_9, Q_{10}),
(d) a CM bilinear transfer function (BLT) F_4 described in terms of a negative resistance ($R_N = -R_L$) where R_L is a resistor load of a current mirror (Q_9, Q_{10}).

In terms of DC analysis, PMOS transistors Q_{11} to Q_{18} and a resistor R_1 form sets of DC current mirrors (Q_{11} to Q_{18}, R_1) for the current-steering circuits and therefore provide DC currents I, 2I or G_0I for F_1, F_2 or F_3 where G_0 is an appropriate gain factor. A resistor R_L provides a DC current G_0I to the output of F_3 where G_0 is an appropriate gain factor.

In terms of small-signal (SS) analysis, the four CM filters F_1, F_2, F_3 and F_4 can be described in terms of current gains $F_1(s)$, $F_2(s)$, $F_3(s)$ and $F_4(s)$, respectively, where the physical frequencies $s = j\omega$. Firstly, the current gain $F_1(s) = i_{O1} / i_{in}$ where i_{in} and i_{O1} are input and output SS currents of F_1 at nodes N and S, respectively. Secondly, the current gain $F_2(s) = i_{O2} / i_{O1}$ where i_{O1} and i_{O2} are input and output SS currents of F_2 at nodes N′ and S′, respectively. Thirdly, the current gain $F_3(s) = i_{O3} / i_{O2}$ where i_{O2} and i_{O3} are input and output SS currents of F_3 at nodes T and U, respectively. Finally, as will be seen later in Section IID, the current gain $F_4(s) = i_{in} / i_{O3}$ of filter F_4 is a bilinear transfer function where i_{O3} and i_{in} are input and output SS currents of F_4 at node N. It can be seen from Fig. 2 that the circuits are all simple current mirrors.

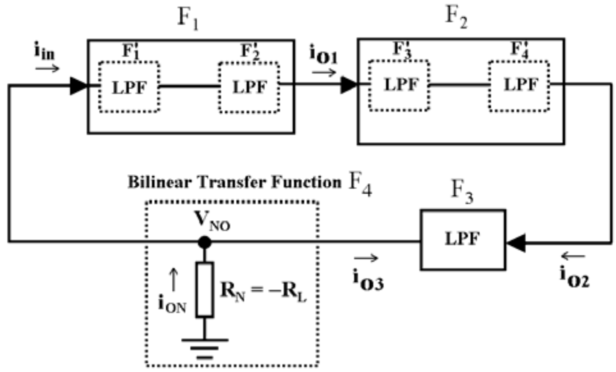

Fig. 1 Small-signal block diagrams of the high-frequency, low-power, CMOS low-pass-filter-based all-current-mirror sinusoidal quadrature oscillator

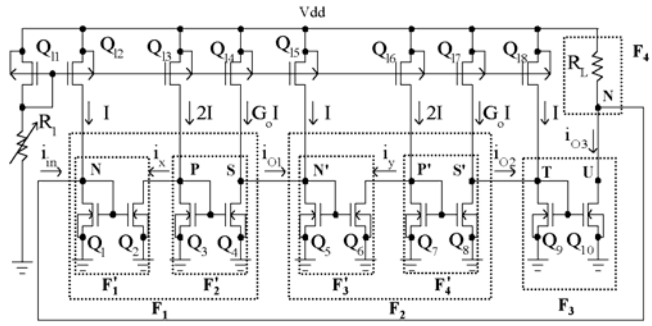

Fig. 2 Circuit diagrams of the high-frequency, low-power, CMOS low-pass-filter-based all-current-mirror sinusoidal quadrature oscillator

B. Current-Mirror Filters F_1, F_2 and F_3

With reference to Fig. 2, let the effect of channel-length modulation of a transistor be negligible. A transconductance g_{mi} of a MOS transistor Q_i for i = 1 to 10 is equal to $g_{mi} = 2I_0/(V_{GSi}-V_T)$ where V_{GSi} is the gate source voltage of Q_i, V_T is the threshold voltage and I_0 is the bias current of Q_i. Table I summarizes the small-signal analysis of the three CM filters F_1, F_2 and F_3 in terms of the small-signal currents i_x, i_y, the output currents i_{O1}, i_{O2}, i_{O3}, the resulting current gains $F_1(s)$, $F_2(s)$, $F_3(s)$ and the internal time constants $\tau_a = C_a / g_{m1}$, $\tau_b = C_b / g_{m3}$, $\tau'_a = C'_a / g_{m5}$, $\tau'_b = C'_b / g_{m7}$ and $\tau_c = C_c / g_{m9}$ where C_a, C_b, C_a', C_b' and C_c are the total internal capacitances at nodes N, P, N′, P′ and T, respectively, of individual current mirrors. The results shown in Table I are provided in the Appendix A1.

TABLE I
CURRENT GAINS OF THE THREE CURRENT-MIRROR (CM) FILTERS F_1, F_2 AND F_3 OF FIG. 2

Filters	Related Currents	Output Currents	Current Gains
F1	$i_x = \frac{i_{in}}{(1+s\tau_a)}$	$i_{O1} = \frac{G_o i_x}{(1+s\tau_b)}$	$F_1(s) = \frac{i_{O1}}{i_{in}} = \frac{G_0}{(1+s\tau_a)(1+s\tau_b)}$
F2	$i_y = \frac{i_{O1}}{(1+s\tau'_a)}$	$i_{O2} = \frac{G_o i_y}{(1+s\tau'_b)}$	$F_2(s) = \frac{i_{O2}}{i_{O1}} = \frac{G_0}{(1+s\tau'_a)(1+s\tau'_b)}$
F3	-	$i_{O3} = \frac{G_0 i_{O2}}{(1+s\tau_c)}$	$F_3(s) = \frac{i_{O3}}{i_{O2}} = \frac{G_0}{(1+s\tau_c)}$

C. Current-Mirror Negative Resistance R_N

By setting $F(s) = F_1(s) \cdot F_2(s) \cdot F_3(s)$, it follows from Table I that

$$\frac{i_{in}}{i_{O3}} = \frac{1}{F(s)} \tag{1}$$

The input current i_{in} to filter F_1 is equal to

$$i_{in} = \frac{v'_{N0}}{Z_{in}} \tag{2}$$

$$Z_{in} = \frac{1/g_{m1}}{(1+s\tau_a)} \tag{3}$$

where Z_{in} is the input impedance of filter F_1 at node N seen by i_{in} (see Appendix A1 for details), v'_{NO} is the small-signal voltage across Z_{in} at node N with respect to node O and node O is the small-signal ground. On the one hand, let i'_{NO} be $i_{O3} + i_{in}$ where i'_{NO} enters node N passing through an impedance Z_1 and then leaves node O. The impedance Z_1 can be found from (1), (2), (3) and i'_{NO} as shown in (4).

$$\frac{v'_{NO}}{i'_{NO}} = \frac{Z_{in}}{1+F(s)} = Z_1 \tag{4}$$

On the other hand, let i_{NO} be a small-signal current that enters node N passing through R_L and then leaves node O. As R_L is a positive resistance, it follows that

$$\frac{v_{NO}}{i_{NO}} = R_L \tag{5}$$

where v_{NO} is the small-signal voltage across R_L at node N with respect to node O. As $i_{NO} = -i_{ON}$, therefore, $R_L = -v_{NO} / i_{ON}$. Both (4) and (5) follow the passive sign convention and therefore v'_{NO} is positive when i'_{NO} is passing through Z_1 and v_{NO} is negative when i_{ON} is passing through R_L. The Kirchhoff's current law at node N yields $i'_{NO} - i_{ON} = 0$ and therefore i'_{NO} in (4) can be substituted with i_{ON}. The Kirchhoff's voltage law around the loop that consists of Z_1 and R_L between nodes N and O yields $-v'_{NO} - v_{NO} = 0$ and therefore v'_{NO} of (4) can be substituted with $-v_{NO}$. It follows from (4) that $v'_{NO} / i'_{NO} = -v_{NO} / i_{ON} = v_{NO} / i_{NO}$. As a result, (4) = (5) and therefore $R_L = Z_{in} / [1 + F(s)]$. Consequently, $i_{in} / i_{O3} = 1 / F(s) = F_4(s)$ where

$$F_4(s) = \frac{-R_N}{(R_N + Z_{in})} \tag{6}$$

$$R_N = -R_L \tag{7}$$

Equation (7) describes a negative resistance $R_N = -(v_{NO} / i_{NO}) = (v_{NO} / i_{ON})$ between nodes N and O, as shown in Fig. 1. It can be seen from (7) that R_N is a simple negative resistance based on an existing resistor R_L of the current mirror (Q_{11}, Q_{12}, R_L).

D. Current-Mirror Bilinear Transfer Function F_4 using Negative Resistance R_N

Equation (6) describes the current gain $F_4(s) = i_{in} / i_{O3}$ of filter F_4 in terms of the negative resistance R_N. Substituting Z_{in} in (6) with (3) yields

$$F_4(s) = -F_5(s) \tag{8}$$

$$F_5(s) = \frac{A_0(1+s\tau_a)}{(1+s\tau_d)} \tag{9}$$

$$A_0 = \frac{g_{m1}R_N}{(1+g_{m1}R_N)} \tag{10}$$

where $\tau_d = A_0\tau_a$. It can be seen from (8), (9) and (10) that $F_4(s)$ is a CM bilinear transfer function.

E. Proposed Low-Pass-Filter-Based All-Current-Mirror Sinusoidal Quadrature Oscillation

It follows from Figs. 1 and 2 that a loop gain $L(s) = F_1(s) \cdot F_2(s) \cdot F_3(s) \cdot F_4(s)$ where $F_1(s)$, $F_2(s)$, $F_3(s)$ are described in Table I and $F_4(s)$ is described in (8) and (9). Therefore $L(s) = -[(G_0)^3(A_0)(1+s\tau_a)]/[(1+s\tau_a)(1+s\tau_b)(1+s\tau'_a)(1+s\tau'_b)(1+s\tau_c)(1+s\tau_d)]$. As τ_b can be equal to τ'_b (i.e. $g_{m1} = g_{m7}$ and $C_b = C_b'$), therefore

$$L(s) = -\frac{(G_0)^3(A_0)}{(1+s\tau_b)^2(1+s\tau'_a)(1+s\tau_c)(1+s\tau_d)} \tag{11}$$

For a sinusoidal oscillation to be sustained at the angular oscillation frequency ω_0, the magnitude $|L(s)|$ and the phase angle $\angle L(s)$ of the loop gain $L(s)$ are equal to unity and zero, respectively. Upon substituting s in (11) with $j\omega_0$ and setting $|L(s)|=1$, therefore the required value of G_0 to sustain steady-state sinusoidal oscillations is equal to

$$G_0 = \sqrt[3]{\frac{(1+\omega_0^2\tau_b^2)^2(1+\omega_0^2\tau_a'^2)(1+\omega_0^2\tau_c^2)(1+\omega_0^2\tau_d^2)}{A_0}} \tag{12}$$

Upon setting $\angle L(s) = 0°$ or $-360°$, it follows that $\angle F_1(s) + \angle F_2(s) + \angle F_3(s) + \angle F_5(s) + 180° = 0°$ where a symbol '$\angle x$' indicates a phase angle of x. Setting $\varnothing_a = \angle F_5(s) + \angle F_1(s)$ and setting $\varnothing_b = \angle F_2(s) + \angle F_3(s)$ yield a quadrature oscillation if

$$\varnothing_a = \varnothing_b = -90° \tag{13}$$

On the one hand, it follows from (13) that $\varnothing_a = \angle F_1(s) + \angle F_5(s) = -90°$ yields the oscillation frequency ω_0

$$\omega_0 = \frac{1}{\tau_b\sqrt{\left(A_0\frac{\tau_a}{\tau_b}\right)}} \tag{14}$$

Analytic treatments for the results shown in (14) are provided in the Appendix A2. On the other hand, it follows from (13) that $\varnothing_b = \angle F_2(s) + \angle F_3(s) = -90°$ yields the oscillation frequency ω_0

$$\omega_0 = \frac{1}{\tau_b}\sqrt{\frac{\tau_b}{\left[\tau_c\left(1+\dfrac{\tau'_a}{\tau_b}\right)+\tau'_a\right]}} \tag{15}$$

Analytic treatments for the results shown in (15) are provided in the Appendix A3. As a result, (14) = (15) and therefore A_0 is equal to

$$A_0 = \frac{\tau_c}{\tau_a}+\left(\frac{\tau'_a\tau_c}{\tau_b\tau_a}\right)+\frac{\tau'_a}{\tau_a} \tag{16}$$

As mentioned earlier in Section IIB, $\tau_a = C_a/g_{m1}$ and $\tau_b = C_b/g_{m3}$, substituting τ_a and τ_b in (14) with ($\tau_a = C_a/g_{m1}$) and ($\tau_b = C_b/g_{m3}$) yields $\omega_0 = (g_{m3}/C_b) / [A_0(C_a/g_{m1})(g_{m3}/C_b)]^{-1/2}$. As τ_a can be equal to τ_b (i.e. $g_{m1} = g_{m3}$ and $C_a = C_b$), therefore

$$\omega_0 = \frac{2I}{\left[\sqrt{\left(A_0\dfrac{C_a}{C_b}\right)}\right](V_{GS3}-V_T)C_b} \tag{17}$$

It can be seen from (17) that ω_0 is tunable through the bias current I. Such an oscillator employs a low-pass-filter-based all-current-mirror technique based on (i) inherent time constants of current mirrors as described in (14) or (17), i.e. the internal capacitances and the transconductance of a diode-connected NMOS, (ii) a simple negative resistance R_N formed by a resistor load R_L of a current mirror as described in (7).

III. Simulation Results

The performance of the circuit shown in Fig. 2 has been simulated through SPICE. As mentioned earlier, transistors are modeled by Alcatel Mietec 0.5 μm CMOS C05MD Technology (AMC) of EUROPRACTICE. The minimum width W and length L of a transistor are 0.8 μm and 0.5 μm, respectively. The unity-gain frequency (f_T) of an NMOS Q_i in this particular example is approximately 7.56 GHz. The supply voltage Vdd = 2 V and R_1 = 18 kΩ. For purposes of simulation, the values of G_0 and R_L are practically chosen to be 1.1 and 14 kΩ, respectively.

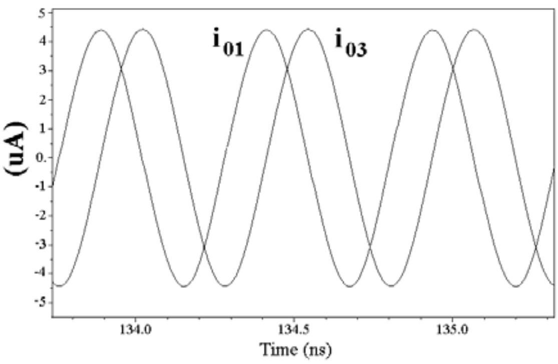

Fig. 3 Oscillograms of quadrature currents i_{O1} and i_{O3} at 1.9 GHz and I = 20 μA

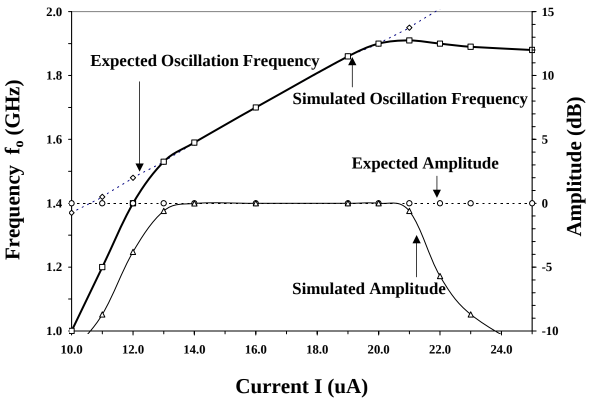

Fig. 4 Plots of the oscillation frequencies and the amplitude of i_{O1} versus bias current I

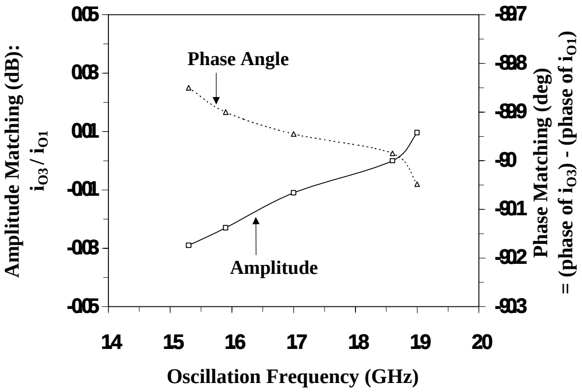

Fig. 5 Amplitude and phase matching of the quadrature signals versus frequency

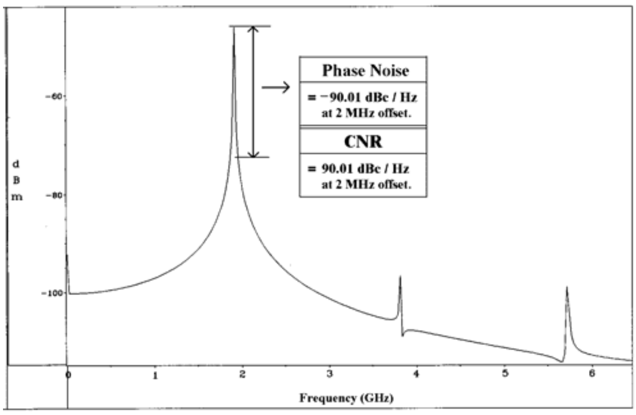

Fig. 6 Harmonic spectrums through FFT of the oscillogram i_{O1} previously depicted Fig. 3 and carrier-to-noise ratio (CNR) = 90.01 dBc/Hz at 2 MHz offset from the 1.9 GHz carrier

Fig. 3 depicts the resulting cosine and sine oscillograms of the quadrature currents i_{O1} and i_{O3}, respectively, at I = 20 μA where the oscillation frequency $f_0 = \omega_0/(2\pi)$ is measured to be 1.9 GHz. Fig. 4 illustrates plots of the oscillation frequencies (GHz) and the amplitudes (dB) of i_{O1} versus bias current I, where the dotted lines indicate the expected analysis and the solid lines indicate the SPICE analysis. As shown in Fig. 4, the oscillation frequencies are tunable over a range from 1.53 to 1.9 GHz by the bias current I from 13 to 20 uA, respectively, and therefore the tuning range is approximately 370 MHz or 21.6%.

Fig. 5 depicts the amplitude matching (dB) in terms of the ratio i_{O3} / i_{O1} as well as the quadrature phase matching (degrees) in terms of ($\theta_{O3}-\theta_{O1}$) of the quadrature currents versus frequency. The amplitude matching is as near as 0.029 dB whilst the quadrature phase matching for −90° is better than 0.15°. Fig. 6 shows the power spectrum levels (dBm) of the fundamental frequency at 1.9 GHz and the next harmonics of the oscillogram i_{O1} previously depicted in Fig. 3 using a commercially available fast Fourier transform (FFT) program. As shown in Fig. 6, the distortions are due mainly to the presence of the second harmonics, which is approximately 51.5 dB down from the fundamental frequency, and they remain essentially at the same magnitude over the entire operational bias-current range (13 μA to 20 μA). Consequently, the total harmonic distortions (THD) are less than 0.3 %.

As shown in Fig. 6, the phase noise is equal to −90.01 [dBc/Hz] at 2 MHz offset from the 1.9 GHz carrier. In other words, CNR = 90.01 dBc/Hz at Δf = 2 MHz and f_0 = 1.9 GHz. It can be seen from Fig. 2 that the total current consumption of the oscillator is equal to $8I + 3G_0I$. For I = 20 μA and G_0 = 1.1, the power dissipation (P_{DC}) is only 0.452 mW. Consequently, the figure of merit [23] called CNR_{norm} = 153.03 dBc/Hz.

IV. Conclusion

The high-frequency low-power all-current-mirror sinusoidal quadrature oscillator has been presented through the use of two 2nd-order low-pass current mirror (CM)-based filters (F_1 and F_2), a 1st-order CM low-pass filter (F_3) and a CM bilinear transfer function (F_4). The bilinear transfer function (F_4) is described in terms of a negative resistance (R_N = -R_L) where R_L is a resistor load of a current mirror. The technique is relatively simple based on (i) inherent time constants of current mirrors, i.e. the internal capacitances and the transconductance of a diode-connected NMOS, (ii) a simple negative resistance R_N formed by a resistor load R_L of a current mirror. Neither external capacitances nor inductances are required.

As a particular example of the second technique, a 1.9-GHz, 0.45-mW, 2-V CMOS low-pass-filter-based all-current-mirror sinusoidal quadrature oscillator has been demonstrated in this Chapter. The oscillation frequency (f_0) is 1.9 GHz and is current-tunable over a range of 370 MHz or 21.6 %. The power consumption is at approximately 0.45 mW. The amplitude matching and the quadrature phase matching are better than 0.05 dB and 0.15°, respectively. Total harmonic distortions (THD) are less than 0.3 %. At 2 MHz offset from the 1.9 GHz, the carrier to noise ratio (CNR) is 90.01 dBc/Hz whilst the figure of merit called a normalized carrier-to-noise ratio (CNR_{norm}) is 153.03 dBc/Hz. The ratio of the oscillation frequency (f_0) to the unity-gain frequency (f_T) of a transistor is 0.25. Comparisons to other approaches have also been included.

Appendix A1

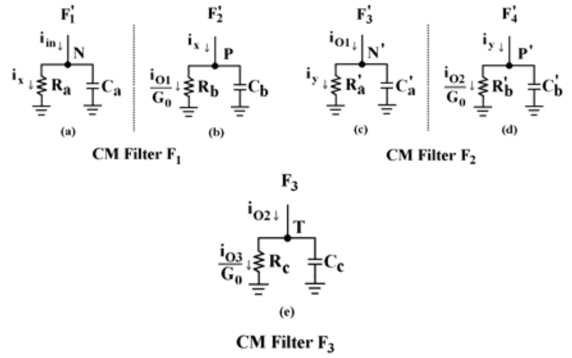

Fig. A1 Input impedances of three current-mirror (CM) filters F_1, F_2 and F_3 : (a) Z_{in} of filter F'_1 at node N, (b) Z_{ini} of filter F'_2 at node P, (c) Z_{inii} of filter F'_3 at node N′, (d) Z_{iniii} of filter F'_4 at node P′ and (e) Z_{iniv} of CM filter F_3 at node T

Appendix A2

Analytical treatments for the results shown in equation (14)

$$\varnothing_a = -90^\circ = \angle F_1(s) + \angle F_5(s)$$

$$-90^\circ = \angle\left[\frac{G_0}{(1+s\tau_a)(1+s\tau_b)}\right] + \angle\left[\frac{A_0(1+s\tau_a)}{(1+s\tau_d)}\right] \;;\; s = j\omega = j\omega_0$$

$$-90^\circ = -\mathrm{Tan}^{-1}(\omega_0\tau_b) - \mathrm{Tan}^{-1}(\omega_0\tau_a) + \mathrm{Tan}^{-1}(\frac{0}{G_0}) + \mathrm{Tan}^{-1}(\frac{0}{A_0}) + \mathrm{Tan}^{-1}(\omega_0\tau_a) - \mathrm{Tan}^{-1}(\omega_0\tau_d)$$

$$90^\circ = \mathrm{Tan}^{-1}(\omega_0\tau_b) + \mathrm{Tan}^{-1}(\omega_0\tau_d) \qquad \text{(A2.1)}$$

$$\mathrm{Tan}^{-1}(\omega_0\tau_b) = A$$
$$\mathrm{Tan}^{-1}(\omega_0\tau_d) = B$$

Take Tan in equation (A2.1);

$$\mathrm{Tan}\ 90^\circ = \mathrm{Tan}\ (A+B)$$

$$\infty = \frac{\mathrm{Tan}\,A + \mathrm{Tan}\,B}{1 - \mathrm{Tan}\,A\,\mathrm{Tan}\,B} \qquad \text{(A2.2)}$$

Therefore equation (A2.2);

$$1 - \mathrm{Tan}\,A\,\mathrm{Tan}\,B = 0 \qquad \text{(A2.3)}$$

Substituting A and B in equation (A2.3);

$$1 - (\omega_0\tau_b)(\omega_0\tau_d) = 0$$
$$1 - \omega_0^2\tau_b\tau_d = 0$$
$$\omega_0^2\tau_b\tau_d = 1 \qquad \text{(A2.4)}$$

Dividing equation (A2.4) with τ_b^2 and rearranging

$$\omega_0^2\frac{\tau_d}{\tau_b} = \frac{1}{\tau_b^2}$$

$$\omega_0^2 = \frac{1}{\tau_b^2\dfrac{\tau_d}{\tau_b}} \quad ; \quad \tau_d = A_0\tau_a$$

$$\omega_0 = \frac{1}{\tau_b\sqrt{\left(A_0\dfrac{\tau_a}{\tau_b}\right)}} \qquad \text{(A2.5)}$$

APPENDIX A3

Analytical treatments for the results shown in equation (15)

$$
\begin{aligned}
\varnothing_b &= -90^\circ = \angle F_2(s) + \angle F_3(s) \\
-90^\circ &= \angle\left[\frac{G_0}{(1+s\tau'_a)(1+s\tau'_b)}\right] + \angle\left[\frac{G_0}{(1+s\tau_c)}\right] \; ; \; s = j\omega = j\omega_0 \\
-90^\circ &= -\mathrm{Tan}^{-1}(\omega_0\tau'_a) - \mathrm{Tan}^{-1}(\omega_0\tau'_b) - \mathrm{Tan}^{-1}(\frac{0}{G_0}) + \mathrm{Tan}^{-1}(\frac{0}{G_0}) \\
&\quad - \mathrm{Tan}^{-1}(\omega_0\tau_c) \\
90^\circ &= \mathrm{Tan}^{-1}(\omega_0\tau'_a) + \mathrm{Tan}^{-1}(\omega_0\tau'_b) + \mathrm{Tan}^{-1}(\omega_0\tau_c) \qquad \text{(A3.1)}
\end{aligned}
$$

$$
\begin{aligned}
\mathrm{Tan}^{-1}(\omega_0\tau'_a) &= C \\
\mathrm{Tan}^{-1}(\omega_0\tau'_b) &= D \\
\mathrm{Tan}^{-1}(\omega_0\tau_c) &= E
\end{aligned}
$$

Take Tan in equation (A3.1);

$$
\begin{aligned}
\mathrm{Tan}\ 90^\circ &= \mathrm{Tan}\ [(C+D)+E] \\
\mathrm{Tan}\ 90^\circ &= \frac{\mathrm{Tan}\,(C+D) + \mathrm{Tan}\,E}{1 - \mathrm{Tan}\,(C+D)\mathrm{Tan}\,E} \\
\infty &= \frac{\left[\dfrac{\mathrm{Tan}\,C + \mathrm{Tan}\,D}{1-\mathrm{Tan}\,C\ \mathrm{Tan}\,D}\right] + \mathrm{Tan}\,E}{1 - \left[\dfrac{\mathrm{Tan}\,C + \mathrm{Tan}\,D}{1-\mathrm{Tan}\,C\ \mathrm{Tan}\,D}\right]\mathrm{Tan}\,E} \qquad \text{(A3.2)}
\end{aligned}
$$

Therefore equation (A3.2);

$$
1 - \left[\frac{\mathrm{Tan}\,C + \mathrm{Tan}\,D}{1-\mathrm{Tan}\,C\ \mathrm{Tan}\,D}\right]\mathrm{Tan}\,E = 0 \qquad \text{(A3.3)}
$$

Substituting C, D and E in equation (A3.3);

$$
\begin{aligned}
1 - \left[\frac{(\omega_0\tau'_a) + (\omega_0\tau'_b)}{1-(\omega_0\tau'_a)(\omega_0\tau'_b)}\right](\omega_0\tau_c) &= 0 \\
1 - \frac{\omega_0^2(\tau'_a + \tau'_b)\tau_c}{(1-\omega_0^2\tau'_a\tau'_b)} &= 0 \\
\omega_0^2(\tau'_a + \tau'_b)\tau_c &= 1 - \omega_0^2\tau'_a\tau'_b \\
\omega_0^2\left[(\tau'_a + \tau'_b)\tau_c + \tau'_a\tau'_b\right] &= 1 \\
\omega_0^2(\tau'_a\tau_c + \tau'_b\tau_c + \tau'_a\tau'_b) &= 1 \qquad \text{(A3.4)}
\end{aligned}
$$

Dividing equation (A3.4) with $\tau_b'^2$ and Rearranging

$$
\begin{aligned}
\omega_0^2\left(\frac{\tau'_a\tau_c}{\tau_b'^2} + \frac{\tau_c}{\tau'_b} + \frac{\tau'_a}{\tau'_b}\right) &= \frac{1}{\tau_b'^2} \\
\omega_0^2\left[\frac{\tau_c}{\tau'_b}(1+\frac{\tau'_a}{\tau'_b}) + \frac{\tau'_a}{\tau'_b}\right] &= \frac{1}{\tau_b'^2} \\
\omega_0^2 &= \frac{1}{\tau_b'^2}\frac{1}{\left[\dfrac{\tau_c}{\tau'_b}(1+\dfrac{\tau'_a}{\tau'_b}) + \dfrac{\tau'_a}{\tau'_b}\right]} \\
\omega_0 &= \frac{1}{\tau'_b}\sqrt{\frac{1}{\left[\dfrac{\tau_c}{\tau'_b}(1+\dfrac{\tau'_a}{\tau'_b}) + \dfrac{\tau'_a}{\tau'_b}\right]}} \quad ; \quad \tau'_b = \tau_b \\
\omega_0 &= \frac{1}{\tau_b}\sqrt{\frac{1}{\left[\dfrac{\tau_c}{\tau_b}(1+\dfrac{\tau'_a}{\tau_b}) + \dfrac{\tau'_a}{\tau_b}\right]}} \\
\omega_0 &= \frac{1}{\tau_b}\sqrt{\frac{\tau_b}{\left[\tau_c\left(1+\dfrac{\tau'_a}{\tau_b}\right) + \tau'_a\right]}} \qquad \text{(A3.5)}
\end{aligned}
$$

REFERENCES

[1] J. Fenk, "Highly Integrated RF-IC's for GSM and DECT Systems-A Status Review," *IEEE Transaction on Microwave Theory and Techniques*, vol. 45 (12), pp. 2531-2539, 1997.

[2] B. Razavi, "Design Considerations for Direct-Conversion Receivers," *IEEE Transaction on Circuits and System-II*, vol. 44, pp. 428-435, 1997.

[3] A. Parssinen, *Direct Conversion Receivers in Wide-Band Systems*, Klumer Academic Plublishers, 2001.

[4] F. Gatta, D. Manstretta, P. Rossi, and F. Svelto, "A Fully Integrated 0.18-µm CMOS Direct Conversion Receiver Front-End with On-Chip LO for UMTS," *IEEE Journal of Solid-State Circuits*, vol. 39(1), pp. 15-23, 2004.

[5] J.B. Hughes, A. Spencer, A. Worapishet, and R. Sitdhikorn, "1 mW CMOS Polyphase Channel Filter for Bluetooth," *IEE Proc.-Circuits Devices Syst.*, vol. 149 (5/6), pp. 348-354, 2002.

[6] D.A. Johns, and K. Martin, *Analog Integrated Circuit Design,* (New York: John Wiley & Sons), 1997.

[7] A. Sedra, and K.C. Smith, *Microelectronic Circuits*, 4th edn., (New York: Oxford University Press), 1998, pp. 984-986 and 441-444.

[8] B. Srisuchinwong, "Fully balanced current-tunable sinusoidal quadrature oscillator," *International Journal of Electronics*, vol. 87, pp. 547-556, 2000.

[9] K. Kumwachara, and W. Surakampontorn, "An Integrable Temperature-Insensitive g_m-RC Quadrature Oscillator," *International Journal of Electronics*, vol. 90 (9), pp. 599-605, 2003.

[10] C. Cakir, U. Cam, and O. Cicekoglu, "Novel Allpass Filter Configuration Employing Single OTRA," *IEEE Transaction on Circuits and System-II: Express Briefs*, vol. 52 (3), pp. 122-125, 2005.

[11] J.W. Horng, H.P. Chou and I.C. Shiu, "Current-mode and Voltage-Mode Quadrature Oscillator Employing Multiple Outputs CCIIs and Grounded Capacitors," *Proceeding of the 2006 IEEE International Symposium on Circuits and Systems*, May 2006.

[12] S. Pookaiyaudom and K. Samootrut, "Current-Mirror Phase-Shifter Oscillator," *Electronics Letters*, vol. 23, pp. 21-23, 1987.

[13] S. Pookaiyaudom and R. Sitdhikorn: "Current-Differencing Band-Pass Filter Realization with Application to High-Frequency Electronically Tunable Low-Supply-Voltage Current-Mirror-Only Oscillator," *IEEE Transaction on Circuits and System-II,* vol. 43, no. 12, pp.832-835, 1996.

[14] S. Pookaiyaudom and J. Mahattanakul, "A 3.3 volt high-frequency capacitorless electronically-tunable log-domain oscillator," *Proceeding of the 1995 IEEE International Symposium on Circuits and Systems,* vol. 2, pp. 829-832, 1995.

[15] A. Leelasantitham and B. Srisuchinwong, "A low-power, high-frequency, all-NMOS all-current-mirror sinusoidal quadrature oscillator," *Microelectronics Journal*, vol. 35, pp. 713-721, 2004.

[16] B. Razavi, "A 1.8 GHz CMOS Voltage-Controlled Oscillator," *Proceedings of the 1997 IEEE International Solid-State Circuits Conference*, pp. 388-389, 1997.

[17] H.-S. Kao and C.-Y. Wu, "A Compact CMOS 2V Low-Power Direct-Conversion Quadrature Modulator Merge with Quadrature Voltage-Controlled Oscillator and RF Amplifier for 1.9GHz RF Transmitter Applications," *Proceedings of the 2000 IEEE International Symposium on Circuits and Systems*, vol. 4, pp. 765-768, 2000.

[18] P. Andreani, "A Low-Phase-Noise Low-Phase-Error 1.8GHz Quadrature CMOS VCO," *Proceedings of the 2002 IEEE International Solid-State Circuits Conference*, vol. 2, pp. 228-229, 2002.

[19] S.B. Anand and B. Razavi, "A CMOS Clock Recovery Circuit for 2.5-Gb/s NRZ Data," *IEEE Journal of Solid-State Circuits*, vol. 36 (3), pp. 432-439, 2001.

[20] D.P. Bautista and M.L. Aranda, "A Low Power and High Speed CMOS Voltage-Controlled Ring Oscillator," *Proceeding of the 2004 IEEE International Symposium on Circuits and Systems*, vol. 4, pp. 752-755, 2004.

[21] J. van der Tang and D. Kasperkovitz, "A 0.9-2.2GHz Monolithic Quadrature Mixer Oscillator for Direct-Conversion Satellite Receivers," *Proceedings of the 1997 IEEE International Solid-State Circuits Conference*, vol. 40, pp. 88-89, 1997.

[22] S. Finocchiaro, G. Palmisano, R. Salerno and C. Sclafani, "Design of Bipolar RF Ring Oscillators," *Proceedings of the 6th IEEE International Conference on Electronics, Circuits and Systems (ICECS'99)*, vol. 1, pp. 5-8, 1999.

[23] W. Sansen, J.H. Huijsing and R.J. van de Plassche (Eds.), *Analog Circuit Design*, Klumer Academic Publishers, 1999, pp. 353-381.